

Synthesis and Characterization of Novel Fused Porphyrinoids Based on Cyclic Carbazole[2]indolones

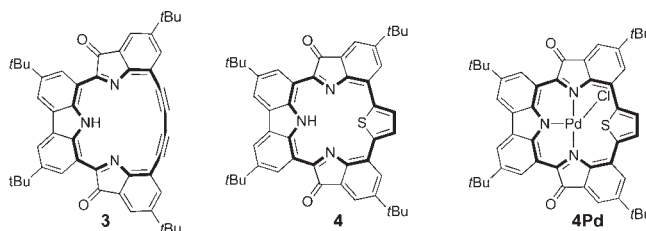
Chihiro Maeda* and Naoki Yoshioka*

Department of Applied Chemistry, Faculty of Science and Technology, Keio University, Kohoku-ku, Yokohama 223-8522, Japan

cmaeda@aplc.keio.ac.jp; yoshioka@aplc.keio.ac.jp

Received March 15, 2012

ABSTRACT



The carbazole- and indolone-based porphyrinoids **3** and **4** were synthesized by stepwise transition-metal-catalyzed coupling reactions. Palladium metalation of **4** produced **4Pd**, which exhibits near-infrared absorption.

Porphyrins are a class of tetrapyrrolic ligands that are of exceptional importance in various biological processes such as photosynthesis, and which also have applications in catalysis, anion sensing, and optical devices.¹ Porphyrins typically absorb strongly in the visible region of the spectrum, although the fusion of additional aromatic rings to the core porphyrin structure results in expanded π -conjugation and additional absorption within the

near-infrared (NIR) region.² Fused porphyrins absorbing in the NIR are anticipated to have applications in photodynamic therapy, since they allow the use of harmless low energy excitation wavelengths, as well as in the production of dye-sensitized solar cells.

Carbazole derivatives have often been studied as novel materials since they are highly emissive, electron conducting, easily modified, and chemically stable.³ Since carbazole is a benzene-fused pyrrole, its incorporation into fused porphyrins presents interesting possibilities. We recently reported the synthesis of the carbazole-based porphyrinoid **1**, which exhibits distinct aromaticity and NIR absorption owing to extended π -conjugation over the macrocycle.⁴

(1) (a) Smith, K. M. In *The Porphyrin Handbook*; Kadish, K. M., Smith, K. M., Guillard, R., Eds.; Academic Press: San Diego, 1999; Vol. 1, Chapter 1, p 1. (b) Lindsey, J. S. In *The Porphyrin Handbook*; Kadish, K. M., Smith, K. M., Guillard, R., Eds.; Academic Press: San Diego, 1999; Vol. 1, Chapter 2, p 45. (c) Smith, K. M. In *The Porphyrin Handbook*; Kadish, K. M., Smith, K. M., Guillard, R., Eds.; Academic Press: San Diego, 1999; Vol. 1, Chapter 3, p 119.

(2) (a) Callot, H. J.; Schaeffer, E.; Cromer, R.; Metz, F. *Tetrahedron* **1990**, *46*, 5253. (b) Crossley, M. J.; Burn, P. L.; Chew, S. S.; Cuttance, F. B.; Newsom, I. A. *J. Chem. Soc., Chem. Commun.* **1991**, 1564. (c) Richeter, S.; Jeandon, C.; Gisselbrecht, J. P.; Ruppert, R.; Callot, H. J. *J. Am. Chem. Soc.* **2002**, *124*, 6168. (d) Tsuda, A.; Osuka, A. *Science* **2001**, *293*, 79. (e) Gill, H. S.; Harmjan, M.; Santamaria, J.; Finger, I.; Scott, M. J. *Angew. Chem., Int. Ed.* **2004**, *43*, 485. (f) Fox, S.; Boyle, R. W. *Chem. Commun.* **2004**, 1322. (g) Yamane, O.; Sugiura, K.; Miyasaka, H.; Nakamura, K.; Fujimoto, T.; Nakamura, K.; Kaneda, T.; Sakata, Y.; Yamashita, M. *Chem. Lett.* **2004**, *33*, 40. (h) Shen, D.-M.; Liu, C.; Chen, Q.-Y. *Chem. Commun.* **2005**, 4982. (i) Kurotobi, K.; Kim, K. S.; Noh, S. B.; Kim, D.; Osuka, A. *Angew. Chem., Int. Ed.* **2006**, *45*, 3944. (j) Davis, N. K. S.; Pawlicki, M.; Anderson, H. L. *Org. Lett.* **2008**, *10*, 3945. (k) Tokuji, S.; Takahashi, Y.; Shinmori, H.; Shinokubo, H.; Osuka, A. *Chem. Commun.* **2009**, 1028. (l) Davis, N. K. S.; Thompson, A. L.; Anderson, H. L. *J. Am. Chem. Soc.* **2011**, *133*, 30.

(3) (a) Grazulevicius, J. V.; Stroehriegl, P.; Pielichowski, J.; Pielichowski, K. *Prog. Polym. Sci.* **2003**, *28*, 1297. (b) Morin, J. F.; Leclere, M.; Ades, D.; Siove, A. *Macromol. Rapid Commun.* **2005**, *26*, 761. (c) Blouin, N.; Leclerc, M. *Acc. Chem. Res.* **2008**, *41*, 1110.

(4) Maeda, C.; Yoneda, T.; Aratani, N.; Yoon, M.-C.; Lim, J. M.; Kim, D.; Yoshioka, N.; Osuka, A. *Angew. Chem., Int. Ed.* **2011**, *50*, 5691.

(5) (a) Piatek, P.; Lynch, V. M.; Sessler, J. L. *J. Am. Chem. Soc.* **2004**, *126*, 16073. (b) Arnold, L.; Norouzi-Arasi, H.; Wagner, M.; Enkelmann, V.; Müllen, K. *Chem. Commun.* **2011**, 970.

(6) Carbazole-containing porphyrins were formed as a consequence of Bergman cyclization of β,β' -diethynylated porphyrins: (a) Aihara, H.; Jaquinod, L.; Nurco, D. J.; Smith, K. M. *Angew. Chem., Int. Ed.* **2001**, *40*, 3439. (b) Nath, M.; Huffman, J. C.; Zaleski, J. M. *J. Am. Chem. Soc.* **2003**, *125*, 11484. (c) Nath, M.; Pink, M.; Zaleski, J. M. *J. Am. Chem. Soc.* **2005**, *127*, 478.

Despite the potential usefulness of such carbazole-based porphyrinoids, only a few examples have been reported to date.^{5,6} Here we report the synthesis of the novel porphyrinoids **2**, **3**, and **4**, containing both carbazole and indole moieties (Figure 1).

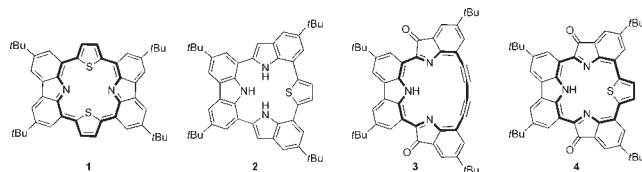


Figure 1. Structures of carbazole-based porphyrinoids **1–4**.

Our synthetic methodology is shown in Scheme 1. The initial intent was to synthesize **2**, which is similar in structure to **1** with regard to the benzo-fused positions, via the annulation reaction of **9** with Na_2S .⁷ In the first synthetic step, starting compound 3,6-di-*tert*-butyl-1,8-bis(trimethylsilylethynyl)carbazole (**5**) was coupled with 4-*tert*-butyl-2,6-diiodoaniline via the Sonogashira reaction⁸ of **6** produced the bis(7-iodoindol-2-yl)-substituted carbazole (**7**). Ethynyl groups were introduced to **7** via the Sonogashira coupling reaction followed by trimethylsilyl deprotection with K_2CO_3 , resulting in **8**. The Glaser coupling reaction of **8** gave a red-colored product, which we expected would be **9**. Spectral analyses, however, established that the product was instead **3**, the oxygen adduct of **9**. High-resolution electrospray-ionization (HR-ESI) mass spectral data show the parent ion peak of **3** at an m/z value of 696.3607 (calcd for $\text{C}_{48}\text{H}_{45}\text{N}_3\text{O}_2$ [$M + \text{H}$]⁺ = 696.3585). Furthermore, the ^{13}C NMR spectrum of this product exhibits a carbonyl peak at $\delta = 194.83$ ppm. Slow diffusion of acetonitrile vapor into a chloroform solution of **3** resulted in the formation of well-defined crystals.

(7) (a) Lagan, J.; Arora, S. K. *J. Org. Chem.* **1983**, *48*, 4317. (b) Krömer, J.; Rios-Carreras, I.; Fuhrmann, G.; Musch, C.; Wunderlin, M.; Debaerdemaeker, T.; Mena-Osteritz, E.; Bäuerle, P. *Angew. Chem., Int. Ed.* **2000**, *39*, 3481. (c) Sumi, N.; Nakanishi, H.; Ueno, S.; Takimiya, K.; Aso, Y.; Otsubo, T. *Bull. Chem. Soc. Jpn.* **2001**, *74*, 979. (d) O'Connor, M. J.; Haley, M. M. *Org. Lett.* **2008**, *10*, 3973.

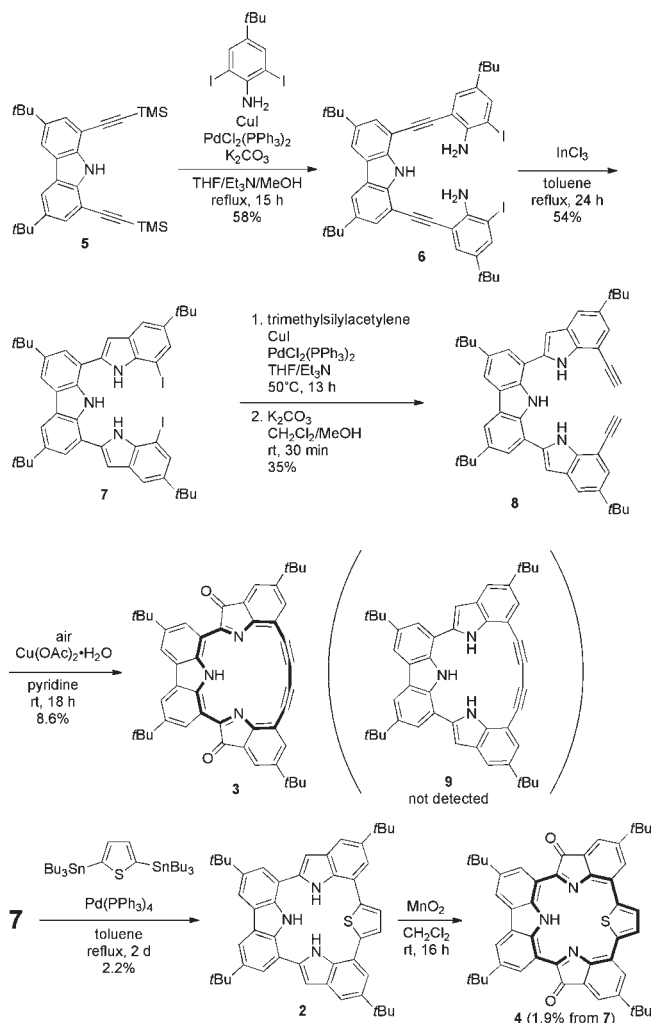
(8) Sakai, M.; Annaka, K.; Fujita, A.; Sato, A.; Konakara, T. *J. Org. Chem.* **2008**, *73*, 4160.

(9) Crystallographic data for **3**: formula $\text{C}_{48}\text{H}_{45}\text{N}_3\text{O}_2$, $M_w = 695.87$, triclinic, space group $P\bar{1}$, $a = 13.6171(3)$, $b = 19.1937(4)$, $c = 20.4913(6)$ Å, $\alpha = 116.6655(10)$, $\beta = 102.6618(10)$, $\gamma = 97.2168(14)^\circ$, $V = 4512.92(19)$ Å³, $Z = 4$, $\rho_{\text{calcd}} = 1.024$ g·cm⁻³, $T = -180$ °C, 4345 measured reflections, 12895 unique reflections ($R_{\text{int}} = 0.0881$), $R_1 = 0.0938$ ($I > 2\sigma(I)$), $wR_2 = 0.2198$ (all data), $\text{GOF} = 1.051$. The contribution to the scattering arising from the presence of disordered solvents in the crystals was removed by using the utility SQUEEZE in the PLATON software package.¹⁴

(10) For examples of indolone-containing porphyrinoids, see: (a) Boyle, R. W.; Dolphin, D. *J. Chem. Soc., Chem. Commun.* **1994**, *21*, 2463. (b) Richeter, S.; Jeandon, C.; Gisselbrecht, J.-P.; Graff, R.; Ruppert, R.; Callot, H. *J. Inorg. Chem.* **2004**, *43*, 251. (c) Smith, K. M.; Vicente, M. G. H. *Sci. Synth.* **2004**, *17*, 1081. (d) Jeandon, C.; Ruppert, R.; Callot, H. *J. Chem. Commun.* **2004**, 1090. (e) Fouchet, J.; Jeandon, C.; Ruppert, R.; Callot, H. *J. Org. Lett.* **2005**, *7*, 5257. (f) Jeandon, C.; Ruppert, R.; Callot, H. *J. Org. Chem.* **2006**, *71*, 3111. (g) Nakamura, S.; Hiroto, S.; Shinokubo, H. *Chem. Sci.* **2012**, *2*, 524.

X-ray diffraction analysis unambiguously demonstrates that the structure of **3** contains indolone units (Figure 2).^{9,10} The mean plane deviation of the macrocycle is 0.083 Å, indicating a highly planar structure. Within the crystal packing structure, molecules of **3** self-stack at intervals of 3.3 Å, as a result of π - π interaction (Figure S11 in the Supporting Information).

Scheme 1. Synthesis of **2**, **3**, and **4**



Additionally, the Stille coupling reaction of **7** with bis(tributylstannyl)thiophene afforded the core modified isophroline **2**. The HR-ESI mass spectrum of **2** shows the parent ion peak at an m/z value of 700.3744 (calcd for $\text{C}_{48}\text{H}_{51}\text{N}_3\text{S}$ [$M - \text{H}$]⁻ = 700.3731). Interestingly, it was found that **2** could be converted into the dioxygenated product **4** through MnO_2 oxidation.

The ^1H NMR spectrum of **3** exhibits a single set of peaks with downfield shifts for carbazole protons (9.32 and 8.82 ppm), indicating a diatropic ring current. Such shifts were not observed for **4** (see the Supporting Information). The UV-vis absorption spectra of **2**, **3**, and **4** are shown in Figure 3. While the spectrum of **2** exhibits absorption primarily in the UV region, the spectra of **3** and **4** are

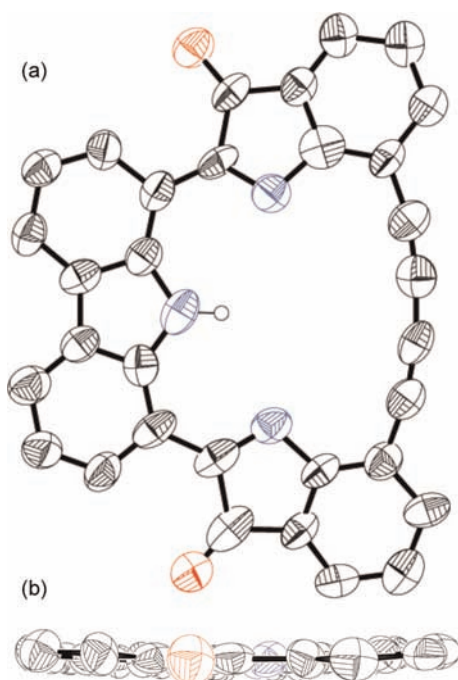


Figure 2. X-ray crystal structure of **3**. *tert*-Butyl groups and hydrogen atoms except for the NH proton are omitted for clarity. The thermal ellipsoids were at a 50% probability level.

considerably broader and extend into the visible region. The addition of TFA to CH_2Cl_2 solutions of either **2**, **3**, or **4** resulted in a significant change in the color of the solutions as a result of red-shifted absorption (Figure S8 in the Supporting Information).

Cyclic voltammetry of **3** and **4** was performed in order to estimate the relatively narrow optical HOMO–LUMO gap. The cyclic voltammogram of **3** exhibits one irreversible oxidation wave (0.73 V) and one reduction wave (–1.06 V), while that of **4** exhibits two reversible oxidation waves (0.40, 0.69 V) and reduction waves (–1.19, –1.30 V) (Figure 4). It is worth noting that the two reversible oxidations and reductions seen with **4** are typical for porphyrinoids, where the electrochemical HOMO–LUMO band gap (1.59 V) is relatively narrow, likely because of extended π -conjugation.

(11) Frisch, M. J.; Trucks, G. W.; Schlegel, H. B.; Scuseria, G. E.; Robb, M. A.; Cheeseman, J. R.; Montgomery, Jr., J. A.; Vreven, T.; Kudin, K. N.; Burant, J. C.; Millam, J. M.; Iyengar, S. S.; Tomasi, J.; Barone, V.; Mennucci, B.; Cossi, M.; Scalmani, G.; Rega, N.; Petersson, G. A.; Nakatsuji, H.; Hada, M.; Ehara, M.; Toyota, K.; Fukuda, R.; Hasegawa, J.; Ishida, M.; Nakajima, T.; Honda, Y.; Kitao, O.; Nakai, H.; Klene, M.; Li, X.; Knox, J. E.; Hratchian, H. P.; Cross, J. B.; Bakken, V.; Adamo, C.; Jaramillo, J.; Gomperts, R.; Stratmann, R. E.; Yazyev, O.; Austin, A. J.; Cammi, R.; Pomelli, C.; Ochterski, J. W.; Ayala, P. Y.; Morokuma, K.; Voth, G. A.; Salvador, P.; Dannenberg, J. J.; Zakrzewski, V. G.; Dapprich, S.; Daniels, A. D.; Strain, M. C.; Farkas, O.; Malick, D. K.; Rabuck, A. D.; Raghavachari, K.; Foresman, J. B.; Ortiz, J. V.; Cui, Q.; Baboul, A. G.; Clifford, S.; Cioslowski, J.; Stefanov, B. B.; Liu, G.; Liashenko, A.; Piskorz, P.; Komaromi, I.; Martin, R. L.; Fox, D. J.; Keith, T.; Al-Laham, M. A.; Peng, C. Y.; Nanayakkara, A.; Challacombe, M.; Gill, P. M. W.; Johnson, B.; Chen, W.; Wong, M. W.; Gonzalez, C.; Pople, J. A. *Gaussian03*, revision B.04; Gaussian, Inc.: Pittsburgh, PA, 2003.

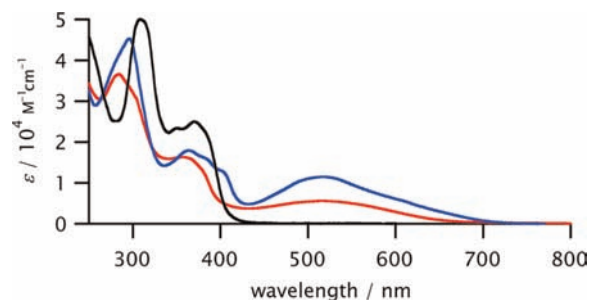


Figure 3. UV–vis absorption spectra in CH_2Cl_2 (black line, **2**; red line, **3**; blue line, **4**).

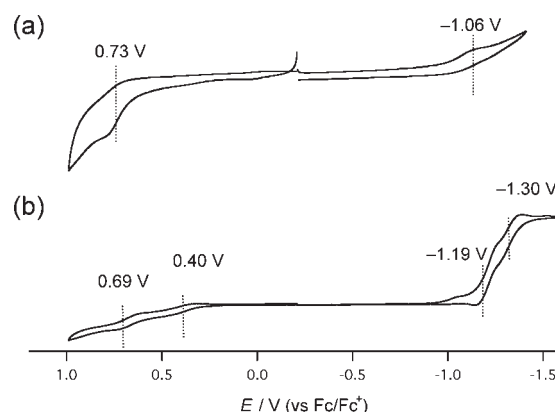


Figure 4. Cyclic voltammograms of (a) **3** and (b) **4** (solvent, CH_2Cl_2 ; supporting electrolyte, Bu_4NPF_6 (0.10 M); counter electrode, Pt; reference electrode, Ag/Ag^+ ; scan rate, 0.01 V/s).

DFT calculations were performed in order to further elucidate the structures and electronic properties of these compounds (Figure 5).¹¹ The calculated HOMO–LUMO gaps of **3** and **4** are narrower than in **2**, which is consistent with the absorption spectroscopy results. Interestingly, the LUMO and LUMO + 1 of **3** and **4** exhibit large electronic coefficients related to the indolone moieties, suggesting that indolones act as an acceptor, and observed broad absorption bands in the visible region are due to intramolecular charge transfer. The NICS values at the center positions of **2** and **4** were calculated to be 2.02, –0.71, respectively, while the values at inner positions of **3** are negative, although the absolute values were not so high. These NICS results, along with the results of ^1H NMR

(12) For examples of metal complexes of monothiaporphyrin, see: (a) Latos-Grażyński, L.; Lisowski, J.; Olmstead, M. M.; Balch, A. L. *Inorg. Chem.* **1989**, *28*, 3328. (b) Pandian, R. P.; Chandrashekar, T. K. *J. Chem. Soc., Dalton Trans.* **1993**, 119. (c) Latos-Grażyński, L.; Lisowski, J.; Chmielewski, P.; Grzeszczuk, M.; Olmstead, M. M.; Balch, A. L. *Inorg. Chem.* **1994**, *33*, 192. (d) Hung, C.-H.; Ou, C.-K.; Lee, G.-H.; Peng, S.-M. *Inorg. Chem.* **2001**, *40*, 6845. (e) Chuang, C.-H.; Ou, C.-K.; Liu, S.-T.; Kumar, A.; Ching, W.-M.; Chiang, P.-C.; dela Rosa, M. A. C.; Hung, C.-H. *Inorg. Chem.* **2011**, *50*, 11947.

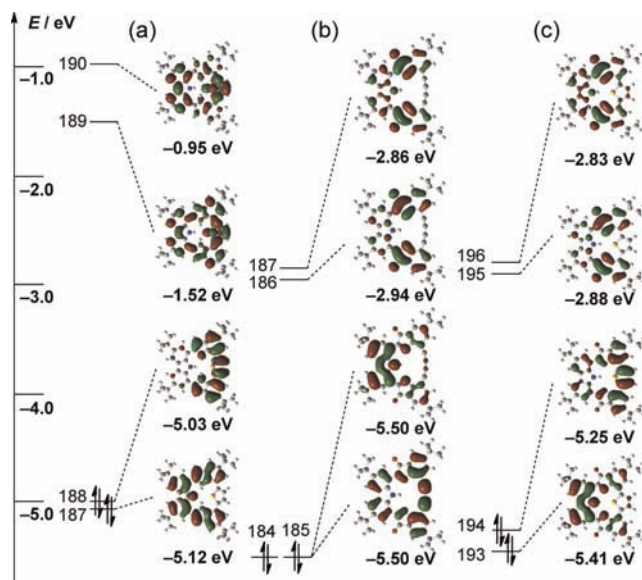


Figure 5. Molecular orbital diagrams of (a) **2**, (b) **3**, and (c) **4** calculated at the B3LYP/6-31G* level.

analysis, indicate that **3** is weakly aromatic, whereas **2** and **4** are essentially nonaromatic. Because the π -conjugation pathways of both **4** and **3** can be considered as 18π -electron systems, **4** will show aromaticity after proper modifications.

The complexation reaction of **4** with palladium was carried out, in order to hinder potential rotation of the thiophene spacer unit.¹² Treatment of **4** with Pd(OAc)₂ and subsequent brine addition afforded the Pd complex **4Pd** (Scheme 2).¹³ The HR-ESI mass spectrum of the product shows a parent ion peak at an m/z value of 834.2390 (calcd for C₄₈H₄₆N₃O₂SPd [$M - \text{Cl}$]⁻ = 834.2356). The UV-vis/NIR absorption spectrum of **4Pd** exhibits a red-shift into the NIR region (Figure 6). The ¹H NMR spectrum of **4Pd** exhibits downfield shifts for the peripheral protons as compared to the spectrum of **4**, indicating a diatropic ring current for **4Pd** (see the Supporting Information). Both the red-shifted absorption and the ring current effect observed for **4Pd** are considered to be due to an increase in structural rigidity of the molecule as a result of the palladium metalation. The cyclic voltammogram of **4Pd** exhibits two reduction waves at -0.92 and -1.19 V, which

(13) Because the ¹H NMR spectrum of **4Pd** is different from that of the crude Pd-complex before brine addition, we assigned the coordination of chloride to Pd center.

(14) (a) Spek, A. L. *PLATON, A Multipurpose Crystallographic Tool*; Utrecht, The Netherlands, 2005. (b) Sluis, P.; van der, Spek, A. L. *Acta Crystallogr., Sect. A* **1990**, *46*, 194.

Scheme 2. Synthesis of **4Pd**

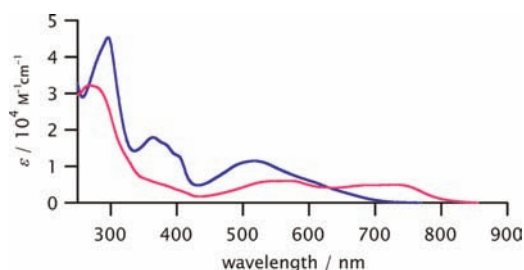
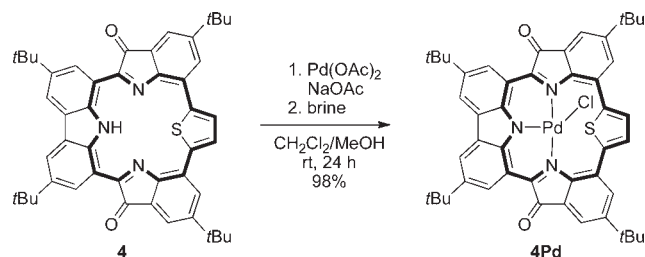


Figure 6. UV-vis/NIR absorption spectra in CH₂Cl₂ (blue line, **4**; pink line, **4Pd**).

is similar to the Pd-complex of a thiaporphyrin (Figure S10 in the Supporting Information).^{12c}

In summary, we have synthesized the novel benzo-fused porphyrinoids **3** and **4**, containing both carbazole and indolone moieties, through metal-mediated synthesis. Furthermore, palladium complexation of **4** afforded **4Pd**, which exhibits weak aromaticity and NIR absorption. Further exploration of novel porphyrinoids and their metal complexes are currently underway in our laboratory.

Acknowledgment. This work was supported by Grants-in-Aid for Young Scientists (No. 23750231 (B)) from MEXT, Japan. We thank Prof. A. Osuka (Kyoto University) for X-ray diffraction analyses and HR-ESI-MS measurements.

Supporting Information Available. Experimental procedures, compound data, and crystallographic data for **3** in CIF format. This material is available free of charge via the Internet at <http://pubs.acs.org>.

The authors declare no competing financial interest.